# Over-current Protection for Series-connected IGBTs based on Desaturation Detection

Lu Yue, Muhammad Abubakr Saeed, Inhwan Lee, and Xiu Yao

Department of Electrical Engineering

State University of New York at Buffalo

Buffalo, USA
luyue@buffalo.edu

Abstract-One major challenge regarding seriesconnected IGBTs is the protection against over-current faults, besides voltage balancing among the devices. In this paper, an over-current protection method based on desaturation detection is proposed for series-connected IGBTs which are controlled by a digital signal processor (DSP) to realize voltage sharing. A hardware test platform was built, which is capable of generating current spikes of various magnitudes and durations. Different aspects of system behavior under fault are characterized to provide design guidance to ensure safety. Finally, experimental results show that the proposed series IGBT control can achieve voltage balance without slowing down the switching transients. Additionally, the desaturation circuit can detect an over-current in less than 1  $\mu s$ . Furthermore, with the proposed protection method, the fault can be fully cleared depending solely on voltage balancing circuits, while maintaining voltage balance during the entire process.

# I. INTRODUCTION

The recent development in high-voltage dc (HVDC) transmission and flexible ac transmission (FACT) requires ever-increasing voltage blocking capabilities from semi-conductor switches. However, current commercial silicon IGBTs can only reach up to 6.5 kV. [1]. Consequently, series-connected IGBTs have been used to replace single devices as switching elements for the voltage-source converters in high-voltage applications.

The major challenge for implementing series IGBTs is the voltage balancing, because the different parameters and parasitic elements in the circuit may cause imbalanced voltage sharing, which can be dangerous for the devices. Extensive research has been done regarding the series IGBT voltage balancing, ranging from passive methods that rely mostly on snubber circuits [2], [3] to active techniques that utilize feedback, such as collectoremitter voltage, gate-emitter voltage, or collector-gate voltage, etc [4], [5]. For this paper, the voltage balancing of the series IGBTs is achieved using the method proposed in [6]. Compared to other active control techniques, it does not require high-speed, high-precision sampling and computing units since the feedback signals

are slow-changing capacitor voltages. What's more, with the method from [6], the IGBTs do not suffer from a slower switching as is sometimes the case with more complicated digital control methods.

Besides voltage balancing, series IGBT protection during faults is another important aspect which requires further investigation. There are two types of faults: opencircuit and over-current faults. This paper focuses on the over-current fault which is the more dangerous type since a high current spike threatens every IGBT in the series string and thus needs to be detected timely. The response time for over-current protection should be within 1  $\mu$ s [7], [8]. Multiple protection techniques have been proposed for single IGBTs in research papers [8]-[10], [13]. di/dt feedback control methods offer fast detection and can be integrated with soft turn-off after a fault detection. However, the circuit is complicated and the detections depend on stray inductance which can be hard to characterize and is sensitive to noises [7], [11]. In this paper, the desaturation detection method is chosen, since it can be realized with a simple and reliable circuit, and the detection is based on the actual fault current which may not be fast-rising [13].

One challenge for series IGBT protection is that if a fault is detected, the entire series branch should turn off in an organized manner. Therefore, passive voltage balancing for series IGBTs [12] is unfit due to the lack of coordination. Contrarily, a central controller can be used to coordinate the IGBT actions during a fault. Another challenge concerns the fault clearing capability. If the series IGBTs are used to form a more complicated topology, such as a voltage source converter (VSC), simply turning off the series IGBTs may not stop the high fault current from flowing through their snubber circuits. Therefore, it is desirable if the series branch can clear the fault under the protection control. In this paper, a DSP is used for both voltage balancing for protection during a fault. Furthermore, an over-current fault generation platform is built, featuring a short-circuit IGBT and an air-core inductor, to inject a controlled current with a ramping rate of a few mega-amps per

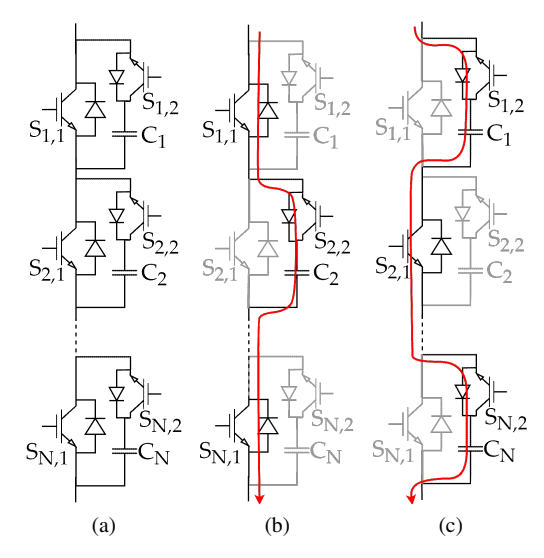


Figure 1: Series IGBT topology and operation principle. (a) main IGBTs and their auxiliary branches, (b) delayed turn-on for  $S_{2,1}$ , (c) delayed turn-off for  $S_{2,1}$ .

second. The short-circuit IGBT is only responsible for injecting the fault current, but not clearing it, to emulate a permanent fault. The fault current is withstood and cleared solely with the series IGBTs and their auxiliary circuits. Additionally, an over-current control scheme for series IGBTs is proposed, which manages to achieve the following goals:

- Fast over-current detection, able to actuate protection and fault clearance mechanisms within 1  $\mu s$  after the fault current exceeds the trip level;
- Safe fault clearance that solely depends on the existing series IGBTs and their auxiliary circuits;
- Voltage balance during and after the fault to keep the IGBTs safe.

Furthermore, balancing controller resolution and related delay length, fault current clearance trajectory, and the resulted shunt capacitor voltage gains are characterized in the paper, which aims to provide guidance during the system design phase and offer explorations into series IGBT protection.

## II. SERIES IGBT CONTROL

## A. System Topology and Operation Modes

Fig. 1a shows the series IGBT circuit topology which consists of two parts. The first part is the main IGBTs connected in series with the annotation  $S_{i,1}$ . The second part is the auxiliary branches, including the auxiliary IGBTs  $S_{i,2}$  and the shunt capacitors  $C_{Si}$ .  $S_{i,1}$  and  $S_{i,2}$  operate in a complementary manner and thus, balancing the main IGBTs' off-state voltages becomes balancing the shunt capacitor voltages [6], [14].

If one IGBT turns on with a delay, such as  $S_{2,1}$  in Fig. 1b, its shunt capacitor stays inserted for a longer

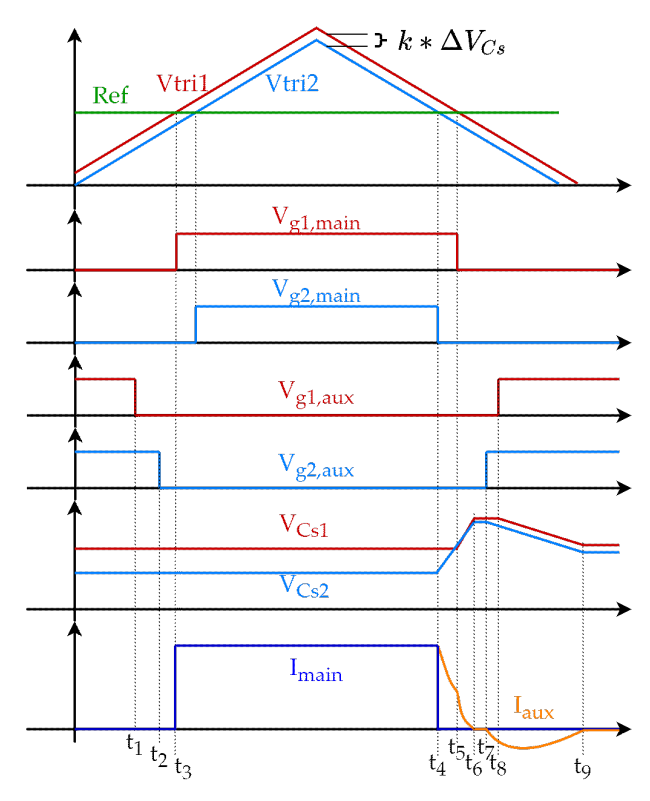


Figure 2: Illustrative waveforms for the voltage balancing control.

time and gets charged more. Therefore, when all the IGBTs are turned on eventually,  $V_{Cs2}$  rises compared to the others. Contrarily, if one module has a delayed turnoff, as shown in Fig. 1c, the corresponding capacitor gets charged less, and its voltage drops. Therefore, by applying gate delays, one can regulate the voltage sharing of the series string.

One way to generate such delays to actively regulate the capacitor voltages is illustrated in Fig. 2. Initially at  $t = 0, V_{Cs1}$  is higher than  $V_{Cs2}$ . Each capacitor voltage is then used to create a dc offset to add to the triangular carrier of the corresponding series module. When the carriers are used to compare with a common reference signal, delays are introduced to the PWM signals. From  $t_1$  to  $t_3$ , the voltage balancing are not affected, since no current charges or discharges the shunt capacitors, as a result of the previous steady-state. At  $t_4$ , the first main IGBT, the one with a lower  $V_C$ , turns off. The falling string current starts to charge the capacitor and raise  $V_{Cs2}$ .  $V_{Cs1}$  also starts to rise after some delay and both capacitor voltages reach their peak when the current falls to 0 at  $t_6$ . The extra charges stored in the capacitors from the falling current will be released when their auxiliary IGBTs turn on at  $t_7$  and  $t_8$ , respectively. This discharge will be over at  $t_9$  and a new steady-state is established.

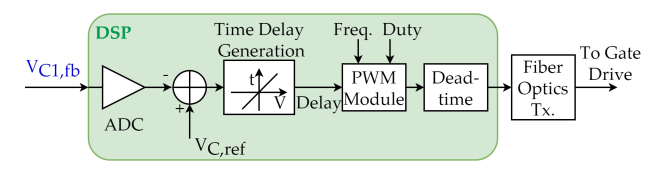


Figure 3: DSP function blocks for series IGBT control.

# B. DSP-based Voltage Balancing Control

The major function blocks are shown in Fig. 3 for implementing the above-mentioned control method with a DSP. The capacitor voltage feedback is sampled with the onboard ADC and its deviation from a reference value is calculated. The error signals are then translated into delays which are then added to the PWM outputs.

The DSP onboard ADC is 12-bit with a reference voltage of 3.3 V, sampling at 50 kHz, which is fast enough given that the target signal,  $V_{Cs}$ , is slow-changing. The shunt capacitors do not fully discharge when main IGBTs are on, since the off-state auxiliary IGBTs block discharging currents. Therefore,  $V_{Cs}$  fluctuates during transients and remain constant during steady-states. The voltage sensor has a gain of 0.0015. Therefore, the ADC's equivalent resolution for the capacitor voltage can be calculated as follows.

$$v_{res} = \frac{V_{ref}}{2^{bit} - 1} * \frac{1}{gain} = 0.54V \tag{1}$$

Furthermore, given that each 1 ms switching cycle is divided into 75000 CPU cycles in the DSP and each bit of ADC input difference is converted to k CPU cycles of delay, the voltage to time delay conversion can be expressed as follows.

$$\Delta t = k * \frac{\Delta V_{CE} Tsw}{75000 * v_{res}} \tag{2}$$

For example, if k = 1 and  $\Delta V_{CE} = 2$  V, the resulting gate delay is 50 ns. However, in the hardware environment, due to noises and feedback loop gain differences, the time delays will fluctuate rather than stay constant even in balanced operation. Nevertheless, with the proposed control, the capacitor voltages will converge to a balanced level and stay so over time.

### III. SERIES IGBT OVER-CURRENT PROTECTION

### A. Desaturation Detection Circuit

Fig. 4 shows the schematic of the desaturation circuit. The inputs are the PWM signal and the IGBT collector voltage which is sensed by  $D_{DE}$ .  $V_C$  plus the forward voltage drop on  $D_{DE}$ ,  $V_{DDE,f}$ , charges  $C_{DE}$  through  $R_2$  when the IGBT is on.  $R_1$  is used to limit the buffer output current and the current flowing into  $D_{DE}$ . MOSFET  $M_1$  generates an inverting logic against the PWM signal and  $M_2$  provides a discharge path for

 $C_{DE}$  when turned on. For  $C_{DE}$ , the charging time constant,  $\tau_1 = R_2 C_{DE}$  is longer than the discharging time constant  $\tau_2 = R_4 C_{DE}$  so that during turn-on there can be blanking time, while during turn-off,  $V_{CDE}$  can quickly reset. Finally, the output stage is a comparator that compares  $V_{CDE}$  with a tunable  $V_{Trip}$  and the output is sent to the DSP via optical transceivers.

When the IGBT turns on,  $D_{DE}$  becomes forward biased,  $V_{CDE}$  charges up to  $V_{C,ON} + V_{DDE,f}$ , and  $M_2$  is open-circuit. During normal operation,  $V_{CDE}$  is lower than  $V_{Trip}$  and Desat\_out remains high. On the other hand, if a high over-current flows through the IGBT,  $V_{CDE}$  will increase and reach  $V_{Trip}$ , flipping the comparator output to low and a detection is made. When IGBT turns off, either during normal operation or by the protection circuit,  $V_C$  will become significantly higher than  $V_{CDE}$  and the voltage drop will be blocked by  $D_{DE}$ . In the meantime,  $M_1$  will turn on  $M_2$  to discharge  $C_{DE}$  quickly.

# B. Over-current Test Platform

The test platform, as shown in Fig. 5, has two series IGBTs,  $S_{1,1}$  and  $S_{2,1}$ . Each IGBT is augmented with an auxiliary branch that consists  $S_{i,2}$  and a 6  $\mu F$   $C_{Si}$ . The power supply is connected to the two series modules via a load resistor. Parallel to the load resistor is the over-current generation branch, consisting of a shortcircuit control switch  $S_{SC}$  and an air-core inductor  $L_{SC}$  which does not saturate at high current levels. A TMS320F28335 DSP serves as the central controller which monitors  $V_{Cs}$  feedbacks via optical fiber and sends trigger signals to the short-circuit switch to start a fault. A desaturation detector is connected between  $S_{2,1}$  collector and emitter and its output is transmitted to the DSP by fiber optics. The optical transceivers have a typical delay of 5 ns and the DSP processing time, after receiving a fault detection signal, is typically 15 ns. Therefore, the signal transmission and processing delays in total are much shorter than 1  $\mu s$  and thus are ignored.

The operation of the hardware platform can be divided into four states when it is used to generate an overcurrent and to protect the series IGBTs from it.

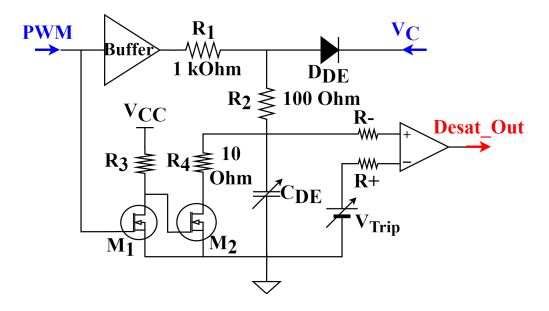


Figure 4: Desaturation circuit schematic.

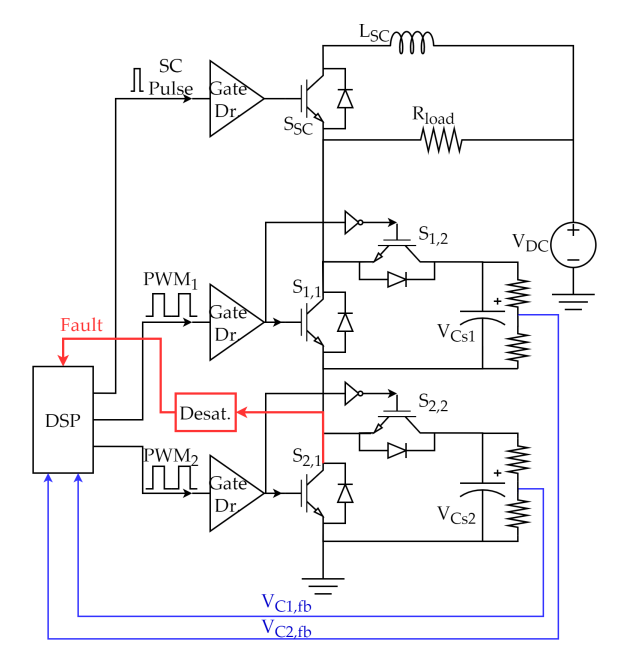


Figure 5: Schematic of the hardware test platform.

- 1) State I: Normal Operation: This is the default operation where all the over-current tests start. In State I, the DSP keeps the voltage sharing balanced. When the main IGBTs  $S_{1,1}$  and  $S_{2,1}$  are on, the branch current is  $I_{load}$ , determined by the source voltage and  $R_{load}$ . When the main IGBTs switch off, the tailing branch current commutes to the auxiliary branches.
- 2) State II: Fault Current Ramp-up: Once the DSP triggers  $S_{SC}$ , the over-current generation branch is connected to the system and the source voltage is imposed across the short-circuit inductor  $L_{SC}$ . The over-current  $I_{SC}$  then starts to ramp up following Eq. 3.

$$I_{SC} = \Sigma L * V_{dc} * t_{fault} \tag{3}$$

where  $\Sigma L$  is the sum of  $L_{SC}$  and stray inductance in the main branch, and  $t_{fault}$  is the duration of the fault until the main IGBTs turn off. Fig. 7 shows Simulink simulation results for  $I_{fault}$  and its ramp-up rate is 6.25 MA/s, determined by  $V_{dc}/\Sigma L$ . The rest of the simulation model parameters can be found in Table I. In the meantime, since all the auxiliary IGBT anti-parallel diodes are reverse biased, the shunt capacitors remain disconnected, maintaining voltages from the previous steady-state. At the end of State II, a fault detection will be made. However, before the main IGBTs start to turn off, the fault current will continue rising.

3) State III: Fault Clearing: This state starts when all the IGBTs have turned off and the fault current starts to commute to the auxiliary branches. A small portion of  $I_{SC}$  will flow through  $R_{load}$ , due to the voltage drop induced by  $L_{SC}$ . However, since it is much smaller

compared to the fault current that charges the shunt capacitors and it does not go through any switches, the resistor current  $I_R$  is ignored.

On the other hand,  $L_{SC}$  and the series shunt capacitors form an LC circuit with an initial current close to the peak  $I_{SC}$ . Therefore,  $I_{SC}$  is subject to the LC resonance and starts to oscillate following the resonance trajectory, as shown in Fig. 7. The resonance frequency can be calculated as follows.

$$f_0 = \frac{1}{T_0} = \frac{1}{2\pi\sqrt{\sum L\frac{C_s}{N}}}$$
 (4)

where N is the number of series modules.

After one-fourth of the resonance cycle, the fault current reaches zero and the fault is cleared because with the proposed method, all the IGBTs are turned off and the auxiliary anti-parallel diodes are reverse biased. Both shunt capacitor voltages increase equally since the dominating factors to  $\Delta V_{Cs1/2}$  are the common fault current and the shunt capacitance rather than stray elements or device parameter differences. The shunt capacitor voltage increase can be calculated using Eq. 5, ignoring the slow damping effect of the load resistor.

$$\Delta V_{Cs} = \frac{1}{C_s} \int_0^{\frac{\pi\sqrt{\Sigma L C_s/N}}{2}} I_0 \cos \frac{t}{\sqrt{\Sigma L C_s/N}} dt$$
$$= I_0 \sqrt{\frac{\Sigma L}{N C_s}}$$
 (5)

where  $I_0$  is the peak fault current through the main IGBTs as well as the auxiliary anti-parallel diodes. In the system design phase, after the device voltage and current margins have been finalized and the parasitic inductance has been evaluated, Eq. 5 can be used to select the number of series IGBTs as well as the shunt capacitance.

4) State IV: Post-fault Protection: After the fault current falls to zero and all the switches are in blocking-state, the voltage sharing of the main IGBTs will be determined by the parasitic capacitances parallel to each IGBT  $C_{CE}$ , as shown in Fig. 6d. Therefore, the voltages may become imbalanced. However, if  $V_{CE}$  of one

Table I: Simulation and Experiment Parameters

Parameter	Value		
$\overline{V_{dc}}$	1 kV		
$L_{SC}$	$160~\mu H$		
$L_{stray}$	$2~\mu H$		
$R_{load}$	320 Ohm		
$C_S$	$6 \mu F$		
$f_{sw}$	1 kHz		
N	2		

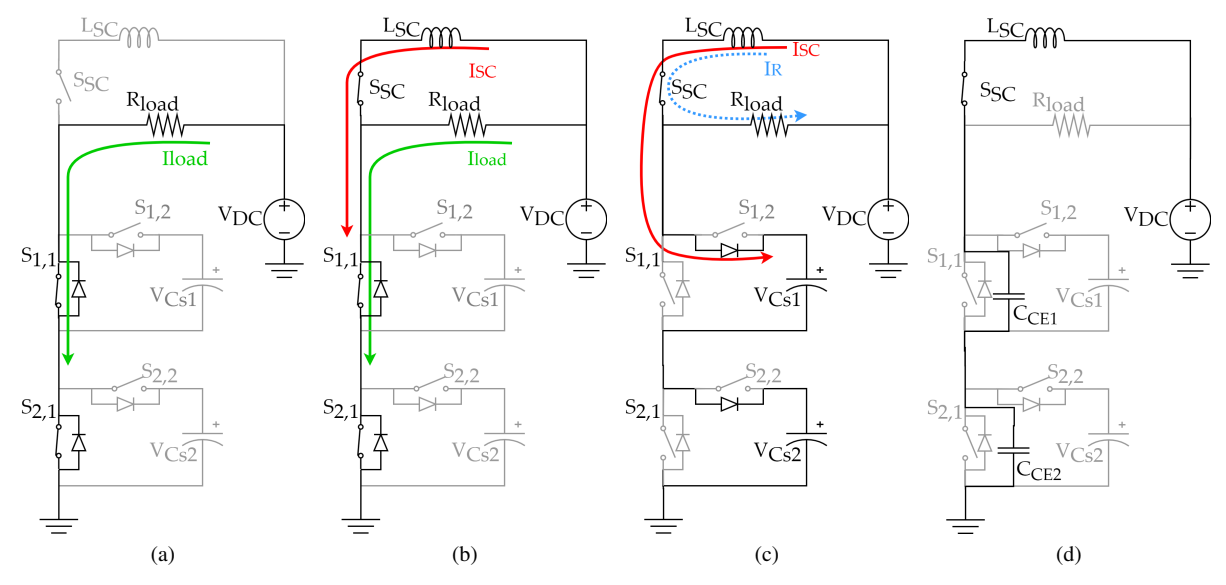


Figure 6: Current paths and inserted components during four operation states. (a) State I: normal operation, (b) State II: fault current ramp-up, (c) State III: fault clearing, (d) State IV: post-fault protection.

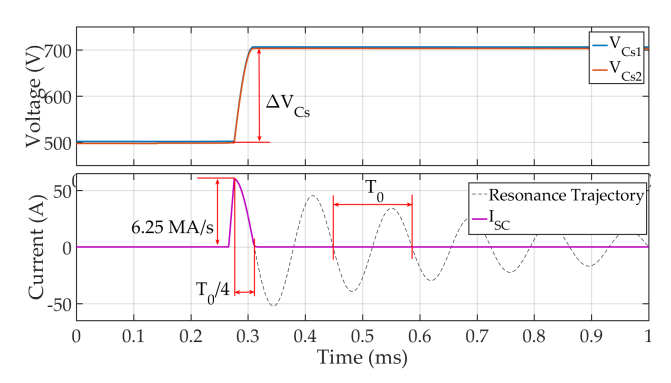


Figure 7: Simulation results for  $V_{Cs}$  and short-circuit current during fault.

main IGBT keeps rising, it will eventually become high enough to forward bias the auxiliary free-wheeling diode and become clamped at the corresponding  $V_{CS}$ . Due to this voltage limiting effect, the series IGBTs will continue to be protected until further measures are taken, such as a system shut down.

### IV. EXPERIMENTAL VALIDATION

The test platform circuit schematic is shown in Fig. 5 and the parameters are listed in Table I. The main and auxiliary IGBTs are IXBH42N170, while the short-circuit control switch is IXGN100N170. In this section, the test results will be presented and discussed first to demonstrate the voltage balancing control, and then series IGBT protection results will be used to illustrate the protection mechanism and its effectiveness.

### A. Series IGBT Voltage Balancing Tests

Before demonstrating the voltage balancing control, series IGBT voltage sharing without it is first investigated. To do so, synchronous gate pulses were sent to the series modules from the DSP and the duty ratio is fixed at 50% without any delay added. The imbalanced voltage sharing waveforms are shown in Fig. 8.

It can be seen that when the dc bus voltage is 1 kV, the  $V_{CE}$  difference between the two series IGBTs is around 100 V or 10% of the bus voltage. The reason for the imbalance is because  $dV_{CE1}/dt$  is higher than  $dV_{CE2}/dt$ , as shown in the zoomed-in transient waveforms. This can be further explained by considering the two series modules and their parasitic capacitances to the ground. The higher ranking series module, or the  $S_{1,1}$  module, has a larger voltage ramp during turnoff transients. Therefore, the parasitic capacitance to the ground in the higher ranking module will draw more current from the gate, which makes  $V_{CE1}$  rise faster than  $V_{CE2}$  [15]. In the turn-on transient, there exists a 20 ns delay between the two collector-emitter voltages. However, the determining factor for the voltage imbalance is still the difference in  $dV_{CE}/dt$ .

The series modules were tested again with voltage balancing control and the results are shown in Fig. 9. From the overall waveforms in Fig. 9a, it can be seen that the  $\Delta V_{CE}$  has reduced greatly from 100 V to 2 V and both series IGBTs share the 1 kV equally. Fig. 9b and 9c show that the delays between  $V_{CE1}$  and  $V_{CE2}$  are 102 ns during turn-off and 38 ns during turn-on. Considering Eq. 1 and 2, the amount of delay is expected for the minor voltage imbalance when k=1. It can also be seen

that the voltage rise and fall times are short, even with a 6  $\mu F$  shunt capacitor, because  $V_{Cs}$  does not connect until  $V_{CE}$  has already reached 500 V. In summary, the voltage balancing control can effectively compensate the voltage imbalance caused by the parasitics in the circuit while not sacrificing the transient performance of the series string.

### B. Over-current Protection

To display the series IGBT over-current protection mechanism, the critical waveforms of the desaturation detection circuit, as well as system behavior, are shown in Fig. 10. The maximum fault current generated in the experiments was 46 A and the IGBTs under test were still considered to be in the saturation region. Considering that a typical IGBT's  $dV_{CE}/dI_{C}$  is smaller in the saturation region than in the desaturation region, an over-current detector capable of detection in the saturation region will be sensitive enough in the desaturation region.

Fig. 10a presents the signal waveforms inside the desaturation detection circuit. At  $t_0$ , the fault occurs and the IGBT collector current  $I_C$  starts to ramp up. In the meantime, the desaturation detection capacitor starts to get charged, since  $V_{CE}$  of the corresponding IGBT is rising, which is reflected in  $V_{CDE}$ . At  $t_1$ , the fault current exceeds the trip value  $I_{trip}$ , and  $V_{CDE}$  reaches the trip voltage. The comparator then pulls the output Detect out to low and the falling edge is used to alarm the DSP of an over-current fault. Upon receiving the falling edge, the DSP sends turn-off signals to all the IGBT gate drives. The time between  $t_1$  and  $t_2$ , which is approximately 0.8  $\mu s$ , is the gate driver processing delay. At  $t_2$ , the gate drivers start turning off all the IGBTs, as shown by the downward bends in  $V_{G1,M}$  and  $V_{G2,M}$ in Fig. 10a. 0.6  $\mu s$  later at  $t_3$ , the main IGBTs have

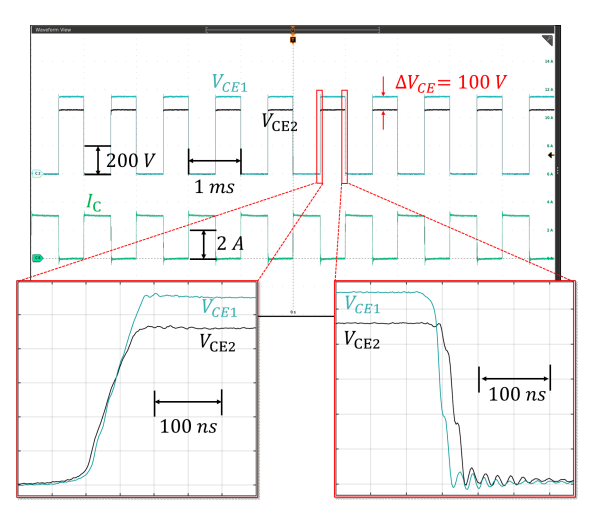
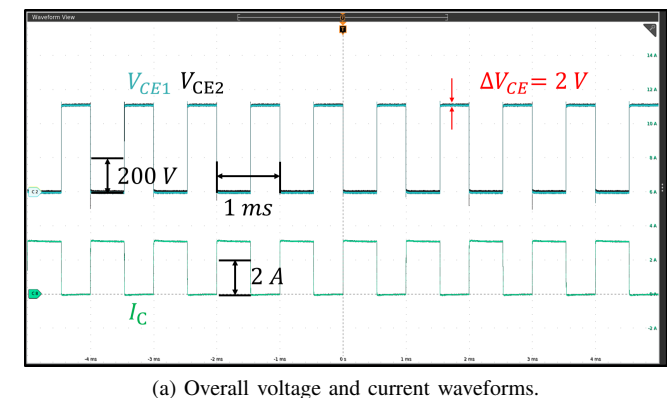


Figure 8: Voltage sharing without balancing control at 1 kV dc bus voltage.



 $\Delta t = 102 \text{ ns}$   $\Delta t_r = 96 \text{ ns}$  1 200 V

(b) Zoomed-in turn-off transient waveforms.  $V_{CE1} V_{CE2}$   $\Delta t = 38 \, ns$   $1 - 200 \, V$   $1 - 300 \, rs$ 

(c) Zoomed-in turn-on transient waveforms.

Figure 9: Voltage and current waveforms of balanced operation at 1 kV dc bus voltage.

finished discharging the miller capacitors and start to cut off the collector current. The fault current then commutes to the auxiliary branches and starts to charge the shunt capacitors now connected in series. The commutation of the fault current from main IGBTs to shunt capacitors causes it to oscillate, as illustrated in Fig. 6c. However, after one-fourth of the oscillation cycle, the fault current becomes below zero at  $t_4$ , as shown in Fig. 10b. Since at this point, all the IGBTs are in blocking-state, no reverse current can flow from the shunt capacitors back to the dc bus, the fault is cleared.

Fig. 10b displays the system behavior under a typical fault which resulted in a 46 A peak fault current. The time between  $t_3$  and  $t_4$  is the fault clearance time. Given that  $L_{SC}$  is 160  $\mu H$  and  $\Sigma C_S$  is 3  $\mu F$ , the clearing time can be calculated by the following equation.

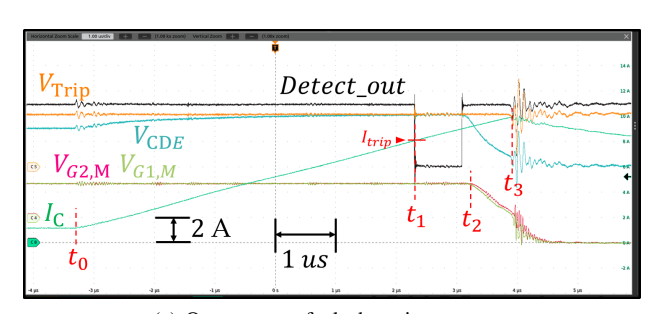
$$t = \frac{\pi}{2} \sqrt{L_{SC} * \Sigma C_S} = 34.4 \mu s \tag{6}$$

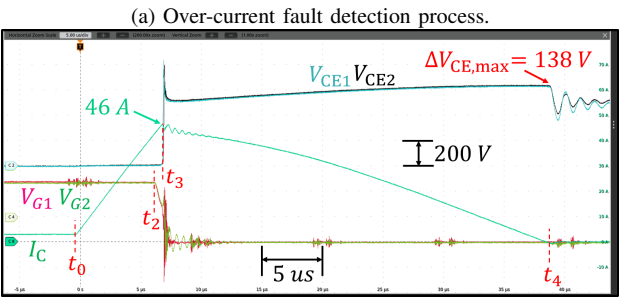
As shown in Fig. 10b, the measured fault clearance time is around 32  $\mu s$ . Fig. 10b also shows that  $V_{CE1}$  and  $V_{CE2}$  can maintain balance from  $t_3$  to  $t_4$ , during which they are determined by the corresponding shunt capacitor voltages.  $V_{CS1}$  and  $V_{CS2}$ , on the other hand, both increase, since they are charged by the falling fault current. Each shunt capacitor voltage gain can be calculated using the equation below which is derived from Eq. 5.

$$\Delta V_{CE} = \frac{1}{C_s} \int_{t_2}^{t_4} i_{fault} dt = 139.2V$$
 (7)

The measured maximum  $\Delta V_{CE}$  in Fig. 10b is 138 V. The shunt capacitors ensure that during a fault, series voltage balance is maintained, because it is determined by the shunt capacitor voltages and the fault current, rather than parasitic capacitance voltages. Furthermore, because of the relatively high capacitance, the shunt capacitors limit the series module voltage gain during a fault.

To further demonstrate the versatility of the proposed over-current detection circuit, a series of tests were done with varying  $V_{Trip}$  and their corresponding trip currents were recorded. The test results are listed in Table II and plotted in Fig. 11. As shown in Table II, changing  $V_t rip$  directly affects the trip current over a wide range. It can also be seen that, even with low fault currents, the proposed detector circuit can still distinguish a fault from normal operation using  $V_{Trip}$ . The graph in Fig. 11 indicates that  $V_{Trip}$  changes with  $I_{Trip}$  following the device I-V curve. Therefore, to select





(b) Fault current and series IGBT voltage sharing during the fault.

Figure 10: Experimental results demonstrating a complete fault detection to clearance process.

Table II:  $V_{Trip}$  and corresponding  $I_{Trip}$ .

$V_{Trip}$ (V)	3.5	3.7	3.8	3.9	4
$I_{Trip}$ (A)	3	4	5.4	8.4	12
$V_{Trip}$ (V)	4.05	4.1	4.15	4.2	
$I_{Trip}$ (A)	14.6	17.2	27.6	37	

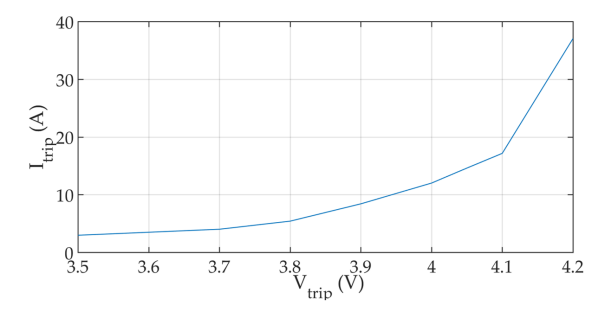


Figure 11: Trip current values based on different trip voltages.

a trip current for the proposed protection circuit, one can refer to the device datasheet and use the corresponding  $V_{CE} + V_{DDE,f}$  as  $V_{Trip}$ .

# V. CONCLUSIONS

This paper proposed an over-current protection method for series-connected IGBTs. The protection method utilizes the outputs of a desaturation detection circuit to alert the DSP which then triggers an organized shutdown of all the IGBTs under fault. The DSP also serves as a central controller responsible for series IGBT voltage balancing which is realized by generating gate delays based on shunt capacitor voltage feedback. Additionally, a test platform capable of generating high current spikes in a controlled way was designed and built. The operation of the test platform was presented and system behaviors, namely fault current and shunt capacitor voltage gain under fault, are characterized. Experimental results show that during normal operation, series IGBTs can achieve balanced voltage sharing without sacrificing transient performance. During a fault, the protection circuit can detect the fault in less than 1  $\mu s$  and react to it in 1.5  $\mu s$ . Furthermore, the fault clearance depends solely on the series IGBTs and their auxiliary circuits, which can simultaneously maintain voltage balance under fault.

# ACKNOWLEDGMENT

This material is based upon work supported by the National Science Foundation under grant no. ECCS 1711659.

### REFERENCES

[1] B. J. Baliga, *The igbt device: design and applications of the insulated gate bioplar transistor*. Binghamton: Elsevier Science & Technology Books, 2015, ch. 20, p. 668.

- [2] J. Chen, J. Lin, and T. Ai, "The techniques of the serial and paralleled igbts," in *Proc. IEEE 22nd International Conference* on *Industrial Electronics, Control, and Instrumentation*, Taipei, Taiwan, 1996, pp. 999 – 1004.
- [3] X. Chen, L. Yu, T. Jiang, H. Tian, K. Huang, and J. Wang, "A fast and series-stacked igbt switch with balanced voltage sharing for pulsed power applications," *IEEE Transactions on Plasma Science*, vol. 45.
- [4] T. Lu, Z. Zhao, J. Shiqi, H. Yu, and L. Yuan, "Active clamping circuit with status feedback for series-connected hv-igbts," *IEEE Transactions on Industry Applications*, vol. 50, no. 5, pp. 3579 – 3590, 2014.
- [5] W. He, P. Palmer, and X. Zhang, "Igbt series connection under active voltage control," in 2011-14th European Conference on Power Electronics and Applications (EPE 2011), Birmingham, UK, Aug. 2011.
- [6] L. Yang, P. Fu, X. Yao, and J. Wang, "A module based self-balanced series connection for igbt," in 2014 IEEE Energy Conversion Congress and Exposition (ECCE), 2014.
- [7] F. F. F. Huang, "Ight fault protection based on di/dt feedback control," in *Proc. IEEE Power Electron. Spec. Conf.*, FL. USA, 2007
- [8] X. Zhang, H.Li, J. Brothers, L. Fu, M. Perales, J. Wu, and J. Wang, "A gate drive with power over fiber-based isolated power supply and comprehensive protection functions for 15-kv sic mosfet," *IEEE Journal of Emerging and Selected Topics in Power Electronics*, vol. 4, no. 3, pp. 946 – 955, Jun. 2016.
- [9] B. Lu and S. K. Sharma, "A literature review of igbt fault diagnostic and protection methods for power inverters," *IEEE Transactions on Industry Applications*, vol. 45, no. 5, pp. 1770– 1777, Sept. 2009.
- [10] U. Choi, F. Blaabjerg, and K. Lee, "Study and handling methods of power igbt module failures in power electronics converter systems," *IEEE Transactions on Power Electronics*, vol. 30, no. 5, pp. 2517–2533, May 2015.
- [11] Z. Wang, X. Shi, L. M. Tolbert, F. Wang, and B. J. Blalock, "A di/dt feedback-based active gate driver for smart switching and fast overcurrent protection of igbt modules," *IEEE Transactions* on *Power Electronics*, vol. 29, no. 7, pp. 3720 – 3732, Jul. 2014.
- [12] R. Chokhawala and S. Sobhani, "Switching voltage transient protection schemes for high current igbt modules," in *Proc. IEEE Applied Power Electronics Conference and Exposition*, 1994, FL. USA, 1994.
- [13] R. Chokhawala, J. Catt, and L. Kiraly, "A discussion on ight short-circuit behavior and fault protection schemes," *IEEE Trans*actions on *Industry Applications*, vol. 31, no. 2, pp. 256 – 263, Apr. 1995.
- [14] L. Yue and X. Yao, "Implementation of a self-balancing control for series igbts," in 2018 IEEE Energy Conversion Congress and Expo (ECCE), Portland, OR, USA, 2018.
- [15] T. V. Nguyen, P. Jeannin, E. Vagnon, D. Frey, and J. Crebier, "Series connection of igbts with self-powering technique and 3d topology," *IEEE Transactions on Industry Applications*, vol. 47, no. 4, pp. 1844 – 1852, May 2011.